AlGaAs/InGaP MBE-grown heterostructures for 1.73eV Solar Cells With 18.7% Efficiency

Ahmed Ben Slimane, Amadeo Michaud, Adrien Bercegol, Julie Goffard, Olivia Mauguin, Xavier Lafosse, Karolien Saliou, Laurent Lombez, Jean-Christophe Harmand, Stéphane Collin

AlGaAs/InGaP MBE-grown heterostructures for 1.73eV Solar Cells With 18.7% Efficiency

Ahmed Ben Slimane[1,2], Amadeo Michaud[3], Adrien Bercegol[1,4], Julie Goffard[1,2], Olivia Mauguin[2], Xavier Lafosse[2], Karolien Saliou[1], Laurent Lombez[1], Jean-Christophe Harmand[2], Stéphane Collin[1,2*]

1 Institut Photovoltaïque d'Ile-de-France (IPVF), Palaiseau, 91120, France

2 Centre de Nanosciences et de Nanotechnologies (C2N), CNRS, Université Paris-Sud/Paris-Saclay, 91120, France

3 TOTAL GRP, Palaiseau, 91120, France

4 EDF R&D, Palaiseau, 91120, France

*stephane.collin@c2n.upsaclay.fr

***Abstract* — Today's most efficient III-V solar cells rely on InGaP materials and are mostly grown by metal organic vapor phase epitaxy (MOVPE). Here, we report on an AlGaAs-based solar cell grown by solid source molecular beam epitaxy (MBE), with a certified conversion efficiency of 18.7%, and a 1.73eV bandgap designed for Si-based dual junction tandem devices. Material characterizations were carried out using Hall effect, secondary-ion mass spectrometry (SIMS) and X-Ray diffraction for the optimization of growth parameters of two conventional homojunction AlGaAs and InGaP solar cells. External quantum efficiencies (EQE) and I-V measurements demonstrate issues related to n-type AlGaAs and p-type InGaP layers. We show an important efficiency increase by merging the best of each structure: a thick p-AlGaAs base with tunable bandgap, and a thin 50 nm InGaP emitter.**

I. Introduction

Silicon photovoltaic technologies are dominating the industry and their development is advancing at a high pace, but Si-based single junction solar cells have an intrinsic conversion efficiency limit of 29.4% [1]. One way to further increase the overall efficiency is to combine silicon with high bandgap materials in a multi-junction design. Therefore, III-V semiconductors have received much attention in the past years. Particularly, AlGaAs and InGaP alloys show great promises for the realization of single junction solar cells with direct bandgaps near 1.72eV, suitable for high efficiency Si-based tandem devices according to detailed balance modeling [2], [3]. Recently, dual junction III-V/Si tandem solar cells have reached efficiencies higher than 30%, with a III-V top cell material based on InGaP [4], [5].

Early research focused on $Al_xGa_{1-x}As$ based alloys because of its bandgap flexibility ranging from 1.42eV to 2.16eV lattice matched to GaAs [6]. This bandgap tunability enables structure design of a fully AlGaAs based solar cell structure. However, AlGaAs alloys suffer from oxygen contamination during growth, limiting its performance [7], [8]. Thus, lattice matched $In_{0.49}Ga_{0.51}P$ grown on GaAs, offered an appealing alternative. InGaP has a relatively good radiation hardness and low interface recombination rate [6], but its bandgap is constrained around 1.9eV with less flexibility as compared to AlGaAs.

Today's record efficiencies of III-V solar cells with bandgaps around 1.7-1.9 eV are dominated by InGaP based structures and are mainly grown by metal organic vapor phase epitaxy (MOVPE). Through careful layer design and bandgap grading, InGaP solar cells reached a record efficiency of 21.4% [9], [10]. However, it is noted that record efficiencies of MBE grown solar cells are lower than those grown with MOVPE. This is largely due to the lower growth temperature in MBE. Nevertheless, improved growth temperature and off-cut substrate resulted in state of the art MBE grown InGaP solar cell with efficiencies up to 16.6% [11]. On the other hand, despite its bandgap flexibility, researchers quickly lost interest in AlGaAs potential due to oxygen contamination during the growth. Best results with AlGaAs cells were achieved by MOVPE, reaching efficiencies of 16.9% for bandgaps near 1.7eV [12], [13].

In this letter, we first investigate two single-junction solar cells made of AlGaAs and InGaP homojunctions grown by MBE. We show that their performances are limited by the material quality of n-AlGaAs and p-InGaP. We propose to combine a thin n-$In_{0.49}Ga_{0.51}P$ emitter with a thick p-$Al_{0.25}Ga_{0.75}As$ base. The resulting heterostructure exhibits a certified efficiency of 18.7% with a bandgap of 1.73eV perfectly suited for III-V/Si tandem solar cells.

II. Experimental procedure

The epitaxial growth of the solar cell structures was performed with a RIBER compact 21 solid-source MBE machine equipped with both arsenic and phosphorous-valved cracker cells. Standard p-type GaAs (100) substrates are used. The growth rates are approximately 1 µm/h for GaAs and $Al_{0.51}GaAs$, and 0.5 µm/h for the other layers. The typical growth conditions are a beam-equivalent pressure (BEP) of

TABLE I

DETAILS OF THE ALGAAS, INGAP AND HETEROJUNCTION GROWTH LAYER STRUCTURES. THE GROWTH IS FROM THE BOTTOM TO THE TOP (N ON P).

Layer type	Thickness (nm)	Doping (cm^{-3})	AlGaAs	InGaP	Heterojunction
Contact	300	1e19	n-GaAs	n-GaAs	n-GaAs
Window	20	5e18	n-$Al_{0.7}GaAs$	n-AlInP	n-AlInP
Emitter	100	1e17	n-$Al_{0.28}GaAs$	n-$In_{0.48}Ga_{0.52}P$	n-$In_{0.48}Ga_{0.52}P$
Base	1000	1e16	p-$Al_{0.28}GaAs$	p- $In_{0.48}Ga_{0.52}P$	p-$Al_{0.28}GaAs$
BSF	20	5e18	p-$Al_{0.7}GaAs$	p-AlInGaP	p-$Al_{0.7}GaAs$
Contact	300	1e19	p-GaAs	p-GaAs	p-GaAs

$1x10^{-5}$ Torr with a V/III ratio of 20 at 550°C for arsenic-based layers, and a V/III ratio of 8 at 500°C for phosphorus-based layers. Beryllium and Silicon were used as p-type and n-type dopants, respectively. Standard photolithography, wet chemical etching, and metal evaporation steps were performed to separate the mesa structures. The size of the solar cells is 0.5 x 0.5 cm^2. The front metal grid is made of Ni/Ge/Au and the full-area back contact on the rear of the substrate is made of Ti/Au. A 65 nm thick SiNx anti-reflective coating (ARC) layer is deposited after the front n-GaAs contact layer is removed by chemical etching using the front electrodes as a mask.

I-V characteristics of the solar cells were measured using a solar simulator providing one-sun AM1.5G irradiance. External quantum efficiency (EQE) measurements were carried out with a Xenon light source, a monochromator, a microscope objective, and contact needles in a four-point contact probe configuration. Si calibrated diodes were used for reference. The J_{sc} is determined from the EQE measurements.

High Resolution X-Ray Diffraction (HRXRD) geometry θ / 2-θ scans were measured at room temperature (25°C) around [0 0 4] reflection peak of GaAs, by means of a multi-configuration X'Pert Pro MRD PANalytical diffractometer with a sealed tube Cu K-α 1 radiation, equipped with an incident beam monochromator Ge (2 2 0)×4. XRDs were performed to determine the lattice mismatch and crystalline properties in InGaP and calibrate Al concentration in AlGaAs, grown on GaAs substrate.

For structure optimization, study of recombination mechanism, band diagrams and doping profiles near interfaces, we used SCAPS, developed by the university of Ghent, Belgium [14].

III. RESULTS AND DISCUSSION

A. AlGaAs and InGaP solar cells

We first optimize the conventional n-p $Al_{0.28}Ga_{0.72}As$ solar cell. We investigate five different structures: (a) our reference sample with a "linear-profile" at interfaces, (b) a "p-i-n" structure where the p-layer is replaced by an intrinsic one, (c) an "abrupt-profile" sample with a growth interruption at interfaces to create a step-like doping and composition profile, (d) a "gradual" Al composition sample, and (e) a "gradual at high-temperature" sample grown at 680°C with a graded Al composition. The growth temperature of our first four samples is 550-570°C. All previous samples have no anti-reflective coating. Their IV-characteristics are plotted in Fig. 1.

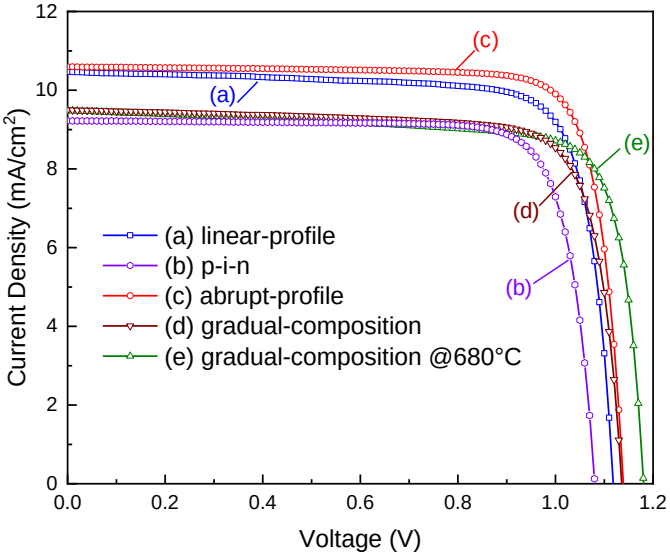

Fig. 1. I-V characteristics of the AlGaAs solar cells without anti-reflective coating: (a) linear-profile, (b) p-i-n, (c) abrupt-profile (d) gradual composition, and (e) gradual composition at 680°C.

Bandgap energy and doping profile were extracted from material characterization carried out using X-ray diffraction, Hall-effect measurements and secondary-ion mass spectrometry (SIMS), EQE and I-V measurements. We observe a lower current collection J_{sc} in the "p-i-n" profile as compared to the "abrupt-profile", due to the better spectral response at longer wavelengths, which is attributed to the decrease of carrier recombination at the base/back surface field (BSF) interface. Further optimization of the intrinsic layer thickness and doping profile is needed. Though, only the "high-temperature" structure (e) exhibits a V_{oc} higher than the "abrupt-profile" (c): this is due to its better material quality. On the other hand, its J_{sc} was lower due to Ga desorption at high temperature leading to an increase of its bandgap and V_{oc}. Also, as a consequence of the gradual composition, potential barriers arise and limit the collection efficiency of generated carriers, resulting in a reduction of the short-circuit current.

"Abrupt profile" is the best AlGaAs solar cell, it is based on an $Al_{0.28}GaAs$ n-p absorber sandwiched between a n-$Al_{0.7}GaAs$

TABLE II

I-V CHARACTERISTICS UNDER 1-SUN AM1.5G SPECTRUM OF SOLAR CELLS WITH AN INGAP HETERO-EMITTER AND AN ALXGA1-XAS BASE OF DIFFERENT ALUMINUM COMPOSITIONS (37%, 28% AND 25%). EG ARE EXTRACTED FROM EQE. ALUMINUM COMPOSITIONS ARE EXTRACTED FROM XRD. NOTE THAT ALL SOLAR CELLS IN THIS TABLE DO NOT HAVE AN ARC.

Al%	E_g (eV)	J_{sc} (mA/cm^2)	FF (%)	V_{oc} (V)	W_{oc} (V)
37	1.884	8.76	77.70%	1.26	0.624
28	1.771	10.5	81.20%	1.26	0.511
25	1.734	12.08	82.15%	1.247	0.487

window layer and a p-$Al_{0.7}GaAs$ BSF layer. The complete stack is described in Table I. The improved structure has an efficiency of η=9.93% with a J_{sc}=10.62 mA/cm^2, V_{oc}=1.14V and FF=82.05%, with no ARC. It is worth mentioning that this efficiency is low compared to state of the art solar cells.

We then optimized independently the growth parameters of InGaP homojunction solar cells. Time resolved fluorescence imaging (TR-FLIM), scanning transmission electrons microscopy (STEM) and room temperature photoluminescence (PL) characterizations were carried out on different InGaP structures while varying the growth temperature and the phosphourous' beam equivalent pressure. We observed a limited efficiency performance in InGaP devices grown by MBE, and we identified the Beryllium (Be) doped layer as the limiting factor. Detailed results of this study are presented elsewhere by Michaud *et al*. The optimized stack is based on a n-p $In_{0.49}Ga_{0.51}P$ homojunction with a slightly higher bandgap, a phosphorus-based n-AlInP window layer and a p-AlInGaP BSF layer (structure detailed in Table I), and has an efficiency of η=9.66% (no ARC).

In the following we compare homojunction AlGaAs and InGaP solar cells. The EQE of the AlGaAs cell, in Fig .2, exhibits a strong drop at short wavelengths (below 500nm). The total J_{sc} difference between the AlGaAs and the InGaP in this spectral region accounts for 0.41 mA.cm^{-2}. The low collection efficiency in the top emitter n-$Al_{0.28}GaAs$ layer is attributed to DX-centers related to the Si doping [15]. They result in a high density of deep defects, which act as non-radiative recombination centers and reduce the minority carrier lifetime and mobility [16]. This issue can be addressed by lowering the Al composition, or by using a Se dopant for this n-type $Al_{0.28}GaAs$ layer [15].

In Fig. 2, the decrease of the EQE of the InGaP in the long-wavelength range (above 500nm) is an indication of collection issues in the base layer. The J_{sc} loss in the longer wavelength region calculated from InGaP and AlGaAs EQEs is equivalent to 3.81 mA.cm^{-2}. It is known that the material quality of p-InGaP for solar cell application is limited by carrier mobilities and the choice of dopants. In fact, cracked phosphorous used in MBE growth induces a significant n-type residual doping, up to 1e16 cm^{-3}, limiting the control of low p-type doping levels in InGaP structures to concentrations higher than ~1e17 cm-3, thus decreasing carriers mobilities, as seen previously by Haegel *et al* and confirmed by Hall effect measurements [17]. Moreover, Be doping in InGaP promotes Oxygen (O) incorporation and increases non-radiative recombination [18].

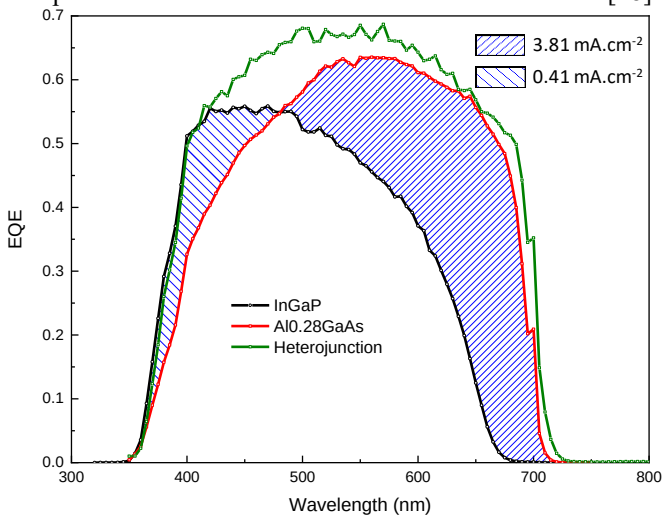

Fig. 2. External quantum efficiency (EQE) of the InGaP (black) and AlGaAs (red) solar cells. The shaded part is the Jsc loss between the InGaP and AlGaAs cells in the designated wavelength area. Structures without ARC.

B. Heterojunction and Aluminum composition

The limitations of previous AlGaAs and InGaP homojunctions, related to the poor quality of n-AlGaAs and p-InGaP, respectively, can be overcome by combining the best of each structure. It results in a heterojunction made of a thick p-AlGaAs base with a bandgap that can be tuned with the Al content, and a thin n-InGaP with a slightly higher bandgap, as described in Table I. The heterostructure relies on a p-AlGaAs base with better carrier mobilities than the p-InGaP, and a n-InGaP emitter for *passivation* purposes and lower DX centers densities than the n-AlGaAs. The spectral response of the p-$Al_{0.28}GaAs$/n-$In_{0.48}Ga_{0.52}P$ heterojunction, shown in Fig. 2, evidences a high collection of carriers at both short and long wavelengths, allowing the recovery of J_{sc} losses in both structures.

The bandgap tunability of p-AlGaAs base layer in the heterostructure allows to further optimize the solar cell efficiency. Table II shows the evolution of IV characteristics under 1-sun with tuned Al composition 0.37, 0.28 and 0.25 for bandgaps 1.88eV, 1.77eV and 1.73eV, respectively (all other layers are identical, see the heterojunction structure in Table I).

Therefore, by reducing the Al composition, we expect to increase J_{sc} and decrease V_{oc}, as the bandgap decreases allowing the cell to absorb a larger part of the spectrum. Also, material quality will improve due to the reduction of DX centers defects related to Al-content [16], [19]. We also note the decrease of the figure of merit W_{oc} expressed as follows:

$$W_{OC} = \frac{E_g}{q} - V_{OC} \qquad (1)$$

where q and E_g are the elemental charge and the bandgap energy, respectively.

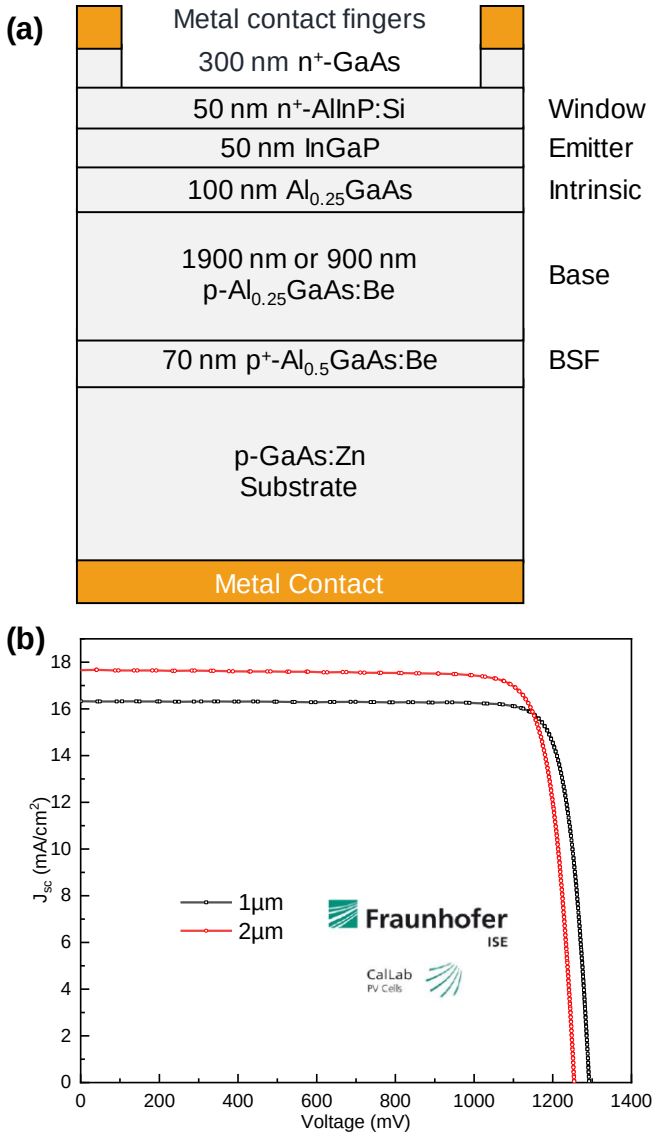

Fig. 3. (a) Layer stack schematic of the optimized heterojunction solar cell (not at scale). Light enters the device from the top. (b) I-V characteristics of the solar cell samples with 1µm thick base (in black) and with 2µm thick base (in red), certified at the Fraunhofer ISE calibration laboratory.

B. Best cell analysis

Finally, our optimized solar cell is the following: a p-$Al_{0.25}GaAs$:Be base with a 1.73 eV direct bandgap, an optimized doping profile at $2x10^{16}$ cm^{-3} and two different thicknesses of 900nm and 1900nm, followed by a thin 100-nm-intrinsic $Al_{0.25}GaAs$ to prevent Be diffusion, and a thin non-doped 50 nm InGaP emitter layer with the highest carrier mobility (the residual doping in the InGaP layer is n-type and has a concentration of $1x10^{16}$ cm^{-3}). The AlGaAs/InGaP heterojunction is sandwiched between a highly doped n-AlInP:Si window layer and a p-$Al_{0.51}GaAs$:Be BSF layer, as described in Fig. 3(a). A 65 nm-thick SiNx anti-reflective coating (ARC) layer is deposited after the front n-GaAs contact layer removal by chemical etching using the front electrodes as a mask. The best cell was measured at the Fraunhofer ISE calibration laboratory under standard test conditions (AM1.5G, 1000 W/m^2, 25°C). We obtained a solar cell with a certified efficiency η=18.7% with J_{sc}=17.6 mA/cm^2, V_{oc}=1.254 V and FF=84.37%, with a base thickness of 2 µm.

In Fig. 3(b), we compare two similar structures with a 1-µm-thick base and a 2-µm-thick base, respectively. We observe an increase of FF in the thinner structure that may be due to the band bending slopes in the thinner base structure and a reduction of bulk recombination. Also, because dark current decreases in thinner absorbers, V_{oc} increases, reaching a W_{oc}=0.438 V, and indicating a good material quality.

IV. Conclusions

We demonstrated that high efficiency AlGaAs solar cells can be grown by MBE, by combining p-AlGaAs base layer with n-InGaP emitter layer, increasing carriers mobilities in the base and reducing DX-centers in the emitter layer. The 18.7% efficiency obtained with a 1.73eV bandgap is a promising result for Si-based tandem devices.

References

[1] A. Richter, M. Hermle, and S. W. Glunz, "Reassessment of the Limiting Efficiency for Crystalline Silicon Solar Cells," *IEEE J. Photovolt.*, vol. 3, no. 4, pp. 1184–1191, Oct. 2013.

[2] T. J. Grassman, J. A. Carlin, C. Ratcliff, D. J. Chmielewski, and S. A. Ringel, "Epitaxially-grown metamorphic GaAsP/Si dual-junction solar cells," in *2013 IEEE 39th Photovoltaic Specialists Conference (PVSC)*, 2013, pp. 0149–0153.

[3] T. Leijtens, K. A. Bush, R. Prasanna, and M. D. McGehee, "Opportunities and challenges for tandem solar cells using metal halide perovskite semiconductors," *Nat. Energy*, vol. 3, no. 10, pp. 828–838, Oct. 2018.

[4] R. Cariou *et al.*, "III–V-on-silicon solar cells reaching 33% photoconversion efficiency in two-terminal configuration," *Nat. Energy*, vol. 3, no. 4, pp. 326–333, Apr. 2018.

[5] S. Essig *et al.*, "Raising the one-sun conversion efficiency of III–V/Si solar cells to 32.8% for two junctions and 35.9% for three junctions," *Nat. Energy*, vol. 2, p. 17144, Aug. 2017.

[6] S. Adachi, *GaAs and Related Materials: Bulk Semiconducting and Superlattice Properties*. WORLD SCIENTIFIC, 1994.
[7] K. Akimoto, M. Kamada, K. Taira, M. Arai, and N. Watanabe, "Photoluminescence killer center in AlGaAs grown by molecular-beam epitaxy," *J. Appl. Phys.*, vol. 59, no. 8, pp. 2833–2836, Apr. 1986.
[8] S. Heckelmann, D. Lackner, F. Dimroth, and A. W. Bett, "Material quality frontiers of MOVPE grown AlGaAs for minority carrier devices," *J. Cryst. Growth*, vol. 464, pp. 49–53, Apr. 2017.
[9] S. Kim, S.-T. Hwang, W. Yoon, and H.-M. Lee, "High performance GaAs solar cell using heterojunction emitter and its further improvement by ELO technique," *32nd Eur. Photovolt. Sol. Energy Conf. Exhib.*, 2016.
[10] M. A. Green, Y. Hishikawa, E. D. Dunlop, D. H. Levi, J. Hohl-Ebinger, and A. W. Y. Ho-Baillie, "Solar cell efficiency tables (version 52)," *Prog. Photovolt. Res. Appl.*, vol. 26, no. 7, pp. 427–436, 2018.
[11] P. Dai *et al.*, "The investigation of GaInP solar cell grown by all-solid MBE," *J. Cryst. Growth*, vol. 378, pp. 604–606, Sep. 2013.
[12] A. Onno, M. Tang, L. Oberbeck, J. Wu, and H. Liu, "Impact of the growth temperature on the performance of 1.70-eV Al0.22Ga0.78As solar cells grown by MBE," *J. Cryst. Growth*, vol. 475, pp. 322–327, Oct. 2017.
[13] S. Heckelmann, D. Lackner, C. Karcher, F. Dimroth, and A. W. Bett, "Investigations on AlxGa1−xAs Solar Cells Grown by MOVPE," *IEEE J. Photovolt.*, vol. 5, no. 1, pp. 446–453, Jan. 2015.
[14] M. Burgelman, P. Nollet, and S. Degrave, "Modelling polycrystalline semiconductor solar cells," *Thin Solid Films*, vol. 361–362, pp. 527–532, Feb. 2000.
[15] K. Takahashi, Y. Minagawa, S. Yamada, and T. Unno, "Improved efficiency of Al0.36Ga0.64As solar cells with a pp−n−n structure," *Sol. Energy Mater. Sol. Cells*, vol. 66, no. 1–4, pp. 525–532, Feb. 2001.
[16] C. Amano, K. Ando, and M. Yamaguchi, "The effect of oxygen on the properties of AlGaAs solar cells grown by molecular-beam epitaxy," *J. Appl. Phys.*, vol. 63, no. 8, pp. 2853–2856, Apr. 1988.
[17] N. M. Haegel *et al.*, "Doping dependence and anisotropy of minority electron mobility in molecular beam epitaxy-grown p type GaInP," *Appl. Phys. Lett.*, vol. 105, no. 20, p. 202116, Nov. 2014.
[18] N. Xiang, A. Tukiainen, M. Pessa, J. Dekker, and J. Likonen, "Oxygen impurities in Ga0.51In0.49P grown by solid-source molecular beam epitaxy," *J. Mater. Sci. Mater. Electron.*, vol. 13, no. 9, pp. 549–552, Sep. 2002.
[19] J. F. Geisz, M. A. Steiner, I. García, S. R. Kurtz, and D. J. Friedman, "Enhanced external radiative efficiency for 20.8% efficient single-junction GaInP solar cells," *Appl. Phys. Lett.*, vol. 103, no. 4, p. 041118, Jul. 2013.